J Membrane Biol (2014) 247:523–530
DOI 10.1007/s00232-014-9662-z

Probing of Various Physiologically Relevant Metals: Amyloid-β Peptide Interactions with a Lipid Membrane-Immobilized Protein Nanopore

Alina Asandei · Sorana Iftemi · Loredana Mereuta · Irina Schiopu · Tudor Luchian

Received: 28 November 2013 / Accepted: 27 March 2014 / Published online: 9 April 2014

Abstract One of the prevailing paradigms regarding the onset of Alzheimer's disease endows metal ions with key roles in certain steps of the amyloid-β (Aβ) peptide aggregation cascade, through peptide conformational changes induced by metal binding. Herein, we focused on the truncated, more soluble $A\beta_{1-16}$ peptide fragment from the human $A\beta_{1-40}$, and demonstrated the utility of a sensing element based on the α-hemolysin (α-HL) protein to examine and compare at single-molecule level the interactions between such peptides and various metals. By using the same approach, we quantified Cu^{2+} and Zn^{2+} binding affinities to the $A\beta_{1-16}$ fragment, whereas the statistical analysis of blockages induced by a single $A\beta_{1-16}$ peptide on the current flow through an open α-HL pore show that the metal propensity to interacting with the peptide and entailing conformational changes obey the following order: $Cu^{2+} > Zn^{2+} > Fe^{3+} > Al^{3+}$.

Keywords Stochastic sensor · Protein pore · Amyloid peptide · Metal sensing

Alina Asandei and Sorana Iftemi have contributed equally to this work.

Electronic supplementary material The online version of this article (doi:10.1007/s00232-014-9662-z) contains supplementary material, which is available to authorized users.

A. Asandei · I. Schiopu
Department of Interdisciplinary Research, Alexandru Ioan Cuza University, Blvd. Carol I, No. 11, 700506 Iasi, Romania

S. Iftemi · L. Mereuta · T. Luchian (✉)
Laboratory of Molecular Biophysics and Medical Physics, Department of Physics, Alexandru Ioan Cuza University, Blvd. Carol I, No. 11, 700506 Iasi, Romania
e-mail: luchian@uaic.ro

Introduction

Amyloid-β (Aβ) peptides are mostly 40 or 42 amino acids long, and their deposition as senile plaques or propensity to disrupt the integrity of cell membranes constitute the essential causes for the manifestation of Alzheimer's disease (AD). In its native conformation, Aβ is unfolded, but conformational transition of the Aβ peptide to a β-sheet-rich state resulting in its aggregation into water-soluble oligomers is believed to be a prerequisite for the onset of AD (Fändrich 2012; Vestergaard et al. 2005).

Currently, it is believed that among other factors, transition metal ions and hydrogen ion homeostasis imbalance influence the aggregation kinetics of Aβ monomers into toxic β-sheet-rich oligomer structures, and metal ions such as copper, zinc, and iron may induce the aggregation of Aβ peptides (Syme et al. 2004; Drew and Barnham 2011; Hung et al. 2010; Leal et al. 2012).

Histidine (His) residues have been suggested to sensitize Aβ to chelating metal ions, and Aβ mutants replacing His residues have been demonstrated to hamper the aggregation-promoting influence of certain metals (Pagel et al. 2008). In more specific terms, it was suggested that Aβ–Cu^{2+} coordination assumes a square-planar arrangement, it involves three intramolecular histidines (i.e., His-6, His-13, and His-14), and the fourth coordinate may be provided by either the amino group of the N-5 terminus, an oxygen from Tyr-10, an oxygen from Glu-3, the carboxylate group of Asp-1, or the amide C=O of Ala-2 (Karr et al. 2005; Stellato et al. 2006; Hong et al. 2010). Apparently, the Aβ–Zn^{2+} complex is more complicated, although a similar coordination as Cu^{2+} has been proposed for Zn^{2+} (Danielsson et al. 2007) or Fe^{3+} chelation (Nair et al. 2010) by Aβ peptides.

Despite remarkable experimental efforts, disparate data exist regarding quantitative estimations of the dissociation

constants for the binding affinity of metal ions to Aβ, with reported values ranging from attomolar to 11 μM for Cu^{2+} and 2–300 μM for Zn^{2+} (Atwood et al. 2000; Tougu et al. 2008). The use of diverse experimental techniques (e.g., far-UV CD, tyrosine, and 4,4_-Bis(1-anilinonaphthalene 8-sulfonate) fluorescence, NMR, EPR, and RAMAN spectroscopies) have paved the way toward characterization of the metal-binding abilities of Aβ, helped revealing the structural features of the Aβ-metal complexes and mapped the structural and dynamic changes upon metal binding (Tougu et al. 2008; Chen et al. 2006, 2011; Curtain et al. 2001; Antzutkin 2004; Smith et al. 2006; Ali et al. 2006). Recent results showed that Zn^{2+} and Al^{3+} increased the hydrophobic exposed protein surfaces, induced higher tyrosine emission, and reduced most residual secondary structures of Aβ. In contrast, Cu^{2+} and Fe^{3+} induced less or did not alter hydrophobic exposed surfaces, decreased tyrosine emission, and reduced residual secondary structures of Aβ, and the stoichiometry of Zn^{2+} or Cu^{2+} to Aβ is 1, and that of Fe^{3+} and Al^{3+} to Aβ may be 2 (Chen et al. 2011).

While $A\beta_{1-40}$ and $A\beta_{1-42}$ are the most prevalent in vivo Aβ forms, in vitro studies of metal interactions with such peptides are often hampered by their high propensity to self-assemble and deposit in amorphous plaques. Therefore, a better strategy for such studies was to employ truncated amyloids containing the minimal metal-binding domain, such as $A\beta_{1-16}$ or $A\beta_{1-28}$, as models to study the thermodynamics of metal binding to Aβ, owing to their relative solubility and stability in the monomeric form. In the Zn^{2+}–$A\beta_{1-16}$ complex, zinc is tetrahedrally coordinated to His-6, His-13, and His-14 through their N-δ1, N-ε2, and N-δ1 atoms, respectively, and to Glu-11 through its O–δ atom, and thermodynamic parameters of Zn^{2+} binding to $A\beta_{1-16}$ indicate a 1:1 binding stoichiometry (Tsvetkov et al. 2010; Istrate et al. 2012; Zirah et al. 2006). Recent data involving isothermal titration calorimetry revealed a 1:1 binding of Cu^{2+} to $A\beta_{1-16}$, which is indicative of a Cu^{2+}-to-peptide ratio of 1:1 (Sacco et al. 2012).

As a powerful alternative to such conventional techniques, either solid-state or protein-based nanopores are excellently suited for investigating molecular interactions at the single-molecule level, due to their versatility with respect to their size, shape, and function. Upon capture within a nanopore, depending on the size and conformation of the specific analyst and the geometry of the nanopore, transient blockades of electrical current with specific kinetics and amplitude can be measured, and subsequent characterization of such individual current blockage events with respect to their amplitude, blockade duration and rate can reveal the identity and concentration of the analyst (Majd et al. 2010; Kasianowicz et al. 2008; Gu and Shim 2010; Bayley et al. 2008). The intrinsic robustness and physico-chemical properties of the α-hemolysin (α-HL) protein secreted by *Staphylococcus aureus* (Song et al. 1996), which upon oligomerization and self-assembly into a target membrane produces a heptameric pore with a minimum diameter of about 1.5 nm, recommends it as an ideal archetype to be used for such purposes (Kasianowicz et al. 1996; Movileanu et al. 2005; Asandei et al. 2011; Gu et al. 1999; Wang et al. 2011). In particular, it has been revealed the potential of protein nanopores to revealing microscopic insights about modulatory effects induced by certain divalent metals on peptides and proteins folding processes (Stefureac et al. 2008; Baran et al. 2010; Mereuta et al. 2012; Wang et al. 2014; Asandei et al. 2013).

In this work, we employed electrical detection on a lipid membrane-immobilized α-HL protein nanopore, to quantify microscopic details underlying the interaction between Cu^{2+}, Zn^{2+}, Al^{3+} and Fe^{3+} and the human amyloid fragment $A\beta_{1-16}$. Our results support the proof-of-concept behind the possibility of using α-HL protein as a novel and potentially useful system to undertake a kinetic analysis of metals—amyloid-β (Aβ) peptide interactions, and estimate the equilibrium constants which characterize the reversible interactions between various metals and peptides.

Materials and Methods

Electrophysiology measurements with protein nanopores were performed on planar lipid membranes made from L-α-phosphatidylcholine obtained as described previously (Asandei et al. 2011). Throughout experiments, both the *cis* (grounded) and *trans* chambers of the bilayer setup contained 2 M KCl, buffered in 10 mM (when the tested metals were either Cu^{2+} or Zn^{2+}) or 50 mM (when the tested metals were either Fe^{3+} or Al^{3+}) HEPES, at pH = 7.3. The elevated HEPES concentration used in the latter cases was necessary in order to better buffer the metal-induced acidity over the range of metal concentrations used in such experiments. Once the successful insertion of a single α-HL heptamer was achieved, upon its *cis*-addition from a protein monomeric solution made in 0.5 M KCl, the $A\beta_{1-16}$ human fragment (Asp–Ala–Glu–Phe–Arg–His–Asp–Ser–Gly–Tyr–Glu–Val–His–His–Gln–Lys) was added in the *trans* side at a 50 μM concentration from a stock solution made in water (1 mM), diluted at the moment of use from a pre-stock solution (10 mM) made in dimethyl sulfoxide. The concentration of the peptide (i.e., 50 μM) was chosen based on our previous experience, as to end up with an optimal event frequency of blockages induced by a single peptide on the α-HL-mediated ion current during control experiments, thus enabling us to properly follow metals effects on the peptide—α-HL reversible interactions. Throughout experiments, and depending upon the metal tested, various metal salts (i.e.,

$CuCl_2$, $ZnCl_2$, $FeCl_3$ and $AlCl_3$) were added in the same side as the peptides (i.e., the *trans* chamber) at incrementally higher concentration. Unless stated otherwise, all reagents used herein were purchased from Sigma-Aldrich, Germany. Measurements were carried out at room temperature ($\sim$23 °C), and the bilayer chamber was housed in a Faraday cage (Warner Instruments, USA), mechanically isolated with a vibration-free platform (BenchMate 2210, Warner Instruments, USA). Ionic current fluctuations, reflecting metal—free or metal—complexed peptides interaction with a single α-HL pore, were recorded in the voltage-clamp mode at an applied potential of $\Delta V = -100$ mV, with an Axopatch 200B (Molecular Devices, USA). Amplified electric signals were low—pass filtered at a corner frequency (f_c) of 10 kHz, and data acquisition was performed using a NI PCI 6221 acquisition board (National Instruments, USA) at a sampling frequency of 50 kHz within the LabVIEW 8.20 (National Instruments, USA). The statistical analysis of average time intervals in-between peptide-induced blockage events (τ_{ON}), and events corresponding to a single α-HL pore temporarily blocked by a peptide (τ_{OFF}), in the absence and the presence of *trans*-added metals at various concentrations, was done as previously reported (Asandei et al. 2011; Mereuta et al. 2012) with the help of the Origin 6 (OriginLab, USA) and pClamp 6.03 (Axon Instruments, USA) software.

Experimental Results and Discussion

In a first set of experiments, we investigated at the unimolecular level the interaction between the *trans*-added $A\beta_{1-16}$ peptides and a single *cis*-added α-HL protein, in the absence and the presence of metals. When added on the *trans* side of a planar lipid membrane containing an inserted α-HL protein, a negative potential in the *trans* side of the membrane facilitate the electrophoretic traffic of the human $A\beta_{1-16}$ peptides toward the α-HL protein, and the ensuing peptide-protein interactions are seen as reversible blockages of the protein-mediated ionic current (Fig. 1, panels a–c). The derivation of the kinetic constants which characterize the non-covalent $A\beta_{1-16}$—α-HL interactions are consistent with a simple bimolecular interaction between the peptide and the pore (Fig. 1, panels d, e), as introduced previously (Movileanu et al. 2005 Asandei et al. 2011).

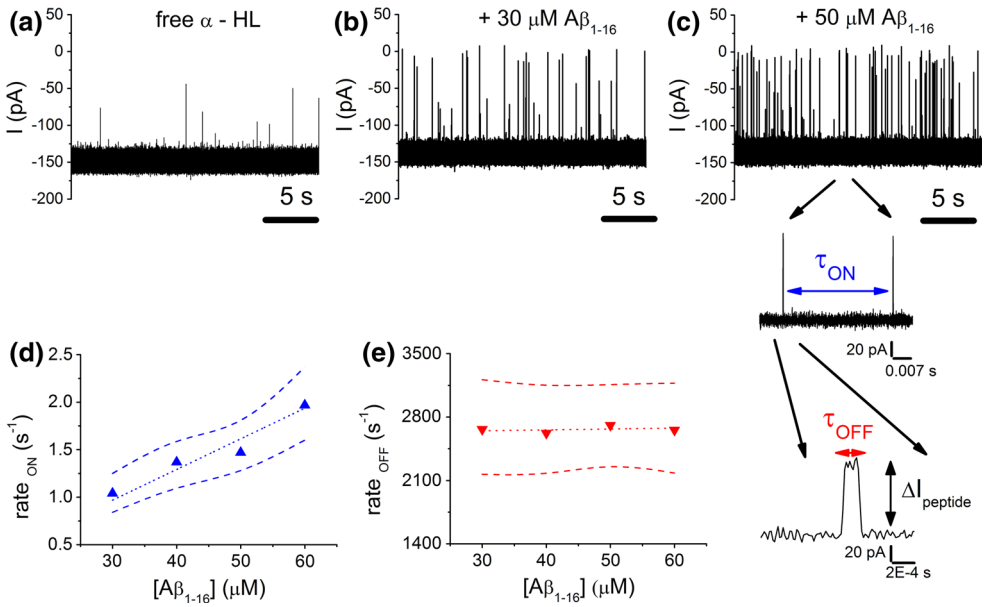

Fig. 1 **a–c** Representative bilayer recordings showing the interaction of a single α-HL protein with $A\beta_{1-16}$ peptides. The α-HL protein was added to the *cis* (grounded) part of the membrane, and all traces were recorded at $\Delta V = -100$ mV, in the presence of peptide added to the *trans* side of the membrane. Inter-event blocking intervals (τ_{ON}) and the blockage duration intervals (τ_{OFF}) were used to derive association and dissociation reaction rates of the α-HL—$A\beta_{1-16}$ reversible interaction within the statistics of exponentially distributed events. The inverse values of average time intervals corresponding to the inter-events seen as temporary blockages provided quantitative estimations of the association rate ($rate_{ON}$, **d**), whereas the inverse values of average blockage events provided the value of dissociation rate ($rate_{OFF}$, **e**), at various concentration values of the added $A\beta_{1-16}$ peptide. The *dashed lines* represent the 95 % confidence intervals for the estimated association ($rate_{ON}$, *triangle*) and dissociation ($rate_{OFF}$, *downward triangle*) reaction rates. The *on* rate constant was obtained from the slope of the linear fit of $rate_{ON}$ versus peptide concentration. The *off* rate constant is independent of $A\beta_{1-16}$ concentration, and it equals $rate_{OFF}$. The zoomed-in representations in panel (**c**) illustrate the representative time intervals that reflect in-between peptide association (τ_{ON}) and transient binding with the open protein pore (τ_{OFF}), whereas the relative current blockage induced by the peptide interaction with a single α-HL is denoted by $\Delta I_{peptide}$

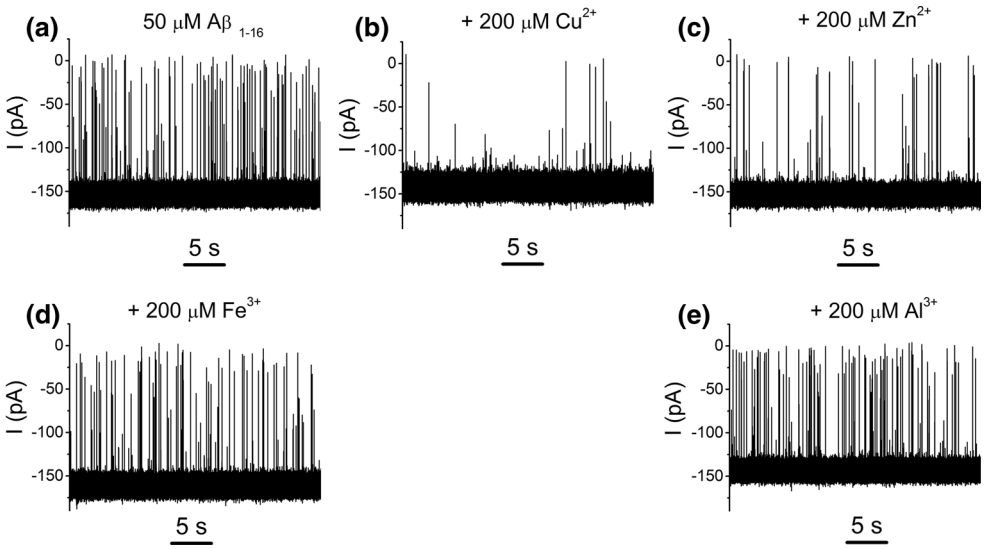

Fig. 2 Typical single-molecule current traces illustrating the reversible interactions between the $A\beta_{1-16}$ peptide and the α-HL pore at $\Delta V = -100$ mV, in the absence (**a**) and the presence of *trans*-added Cu^{2+}, Zn^{2+}, Fe^{3+} and Al^{3+} at 200 μM. Upward current spikes reflect the transient association of a single peptide with the protein pore

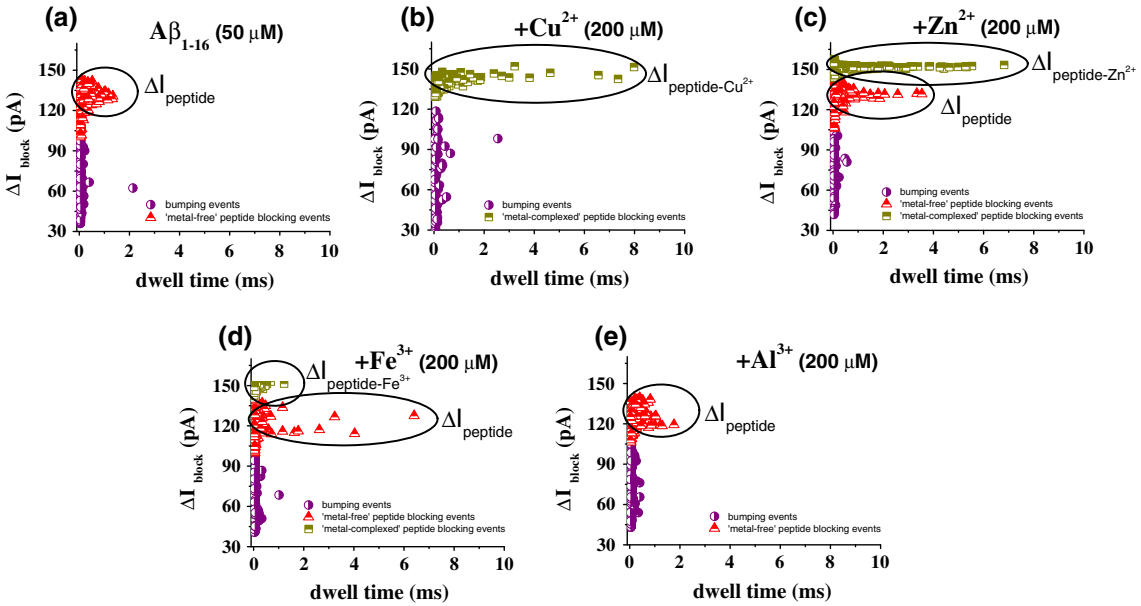

Fig. 3 Scatter-plots of the 'dwell time'–'relative blockage amplitude' joint distributions of various $A\beta_{1-16}$ peptide-induced blockage events, capturing the distinct fingerprint of the blockages induced by such peptides, added in the *trans* side of the membrane at a concentration of 50 μM, on the open-state α-HL current in the absence (**a**), and the presence of 200 μM of various metals (**b**–**e**). The distinct blockage events associated to metal-free ($\Delta I_{peptide}$) and metal-complexed peptides are indicated by the ellipse-like domains. During the kinetic dwell-times analysis, the bumping-like events evidenced through their reduced relative amplitude and low lifetime were excluded from the statistics

During the course of reversible interactions between the human $A\beta_{1-16}$ peptide and a single α-HL pore, the *trans*-chamber addition of Cu^{2+}, Zn^{2+}, Al^{3+}, or Fe^{3+} led to distinct alterations in the kinetic fingerprint of blockade currents induced by the peptide from those in the absence of metals (Fig. 2, panels b–d). At the first glance, from such recordings it appears that unlike Cu^{2+} and Zn^{2+}, addition of Al^{3+} and Fe^{3+} entails a very slight change in the frequency of blockages caused by the $A\beta_{1-16}$ interaction with the α-HL pore.

In the absence of metals, the relative current blockage entailed by the $A\beta_{1-16}$ interaction with a single α-HL pore equals $\Delta I_{peptide} = 132 \pm 1.45$ pA (Fig. 3, panel a). Thus, due to their consistent value seen in experiments performed in the absence or the presence of metals, relative current blockages in the vicinity of this value were attributed to a similar type of interaction, namely between a metal-free $A\beta_{1-16}$ peptide and the protein pore.

It should be remarked that in the presence of relatively high amounts of Cu^{2+} (200 μM), the scatter plots of the

events joint distributions which fingerprints the distribution in the amplitude-time space of the blockage events induced by the peptide on the α-HL, indicate the prevalent presence of one species of the peptide, namely the metal-complexed peptide (Fig. 3, panel b), which induces a current blockage of $\Delta I_{peptide\text{-}Cu}{}^{2+} = 148.00 \pm 1.70$ pA. To a first account and as reported previously (Asandei et al. 2013), we posit that the elevated degree of current obstruction caused by the 'metal-complexed' peptide (vide infra, as well) indicate that such complexes enter the protein lumen, and the metal-induced conformational changes enable them a tighter geometrical fit with the protein lumen than the 'metal-free' peptide.

Notably, a similar concentration of added Zn^{2+} (200 μM) still leaves two species of peptides in the buffer, namely the 'metal-free' and 'metal-complexed' ones, visible through the distinct extent of obstruction of the ion current mediated by a single α-HL pore (Fig. 3, panel c) of $\Delta I_{peptide} = 139 \pm 0.88$ pA and $\Delta I^{2+}_{peptide\text{-}Zn} = 148.86 \pm 0.64$ pA. This observation can be rationalized through the lower affinity of Zn^{2+} to $A\beta_{1-16}$, as compared to Cu^{2+} (vide infra), that precludes the peptide saturation by added Zn^{2+} at 200 μM. As Fig. 3, panel d shows, the same phenomenon is noticeable in the presence of Fe^{3+}, whereby the main blockages seen are attributed to the interaction between the metal-free peptide and the protein pore ($\Delta I_{peptide} = 134 \pm 0.51$pA), and metal-complexed peptide and the protein pore ($\Delta I^{3+}_{peptide\text{-}Fe} = 148.00 \pm 0.53$ pA), and this comes as a supplementary indication of the lower affinity of this metal to $A\beta_{1-16}$ reflected by the kinetic analysis of the blockage events (vide infra). For the case of $A\beta_{1-16}$–Al^{3+} interactions, the scatter plot analysis showed no significant contributions of 'metal-complexed' peptide events to the blockages of ion current mediated by a single α-HL protein, besides those entailed by the protein interaction with 'metal-free' $A\beta_{1-16}$, as the comparison of panels e and a, Fig. 3, reveals.

To investigate in deeper details these observations, we resorted to the detailed kinetic analysis of current blocking events recorded in the presence of various metals added at incrementally higher concentrations in the *trans* chamber. We observed that average time of blockage events that reflects dwell times while single peptide resides on the protein pore (τ_{OFF}) (Fig. 4, panel a), and values of times in-between consecutive peptide-induced blockages events (τ_{ON}) (Fig. 4, panel b), increased monotonically with the concentration of added Cu^{2+} (see also Asandei et al. 2013) and Zn^{2+}, while little change ensued following Fe^{3+} and Al^{3+} addition, in accordance with results shown in Fig. 3. These data demonstrate that in qualitative terms, the propensity of the metals studied to interact with $A\beta_{1-16}$, triggers conformational changes in it, and thus alter the dynamics of reversible $A\beta_{1-16}$—α-HL pore interactions, is concentration-dependent and decreases in the order $Cu^{2+} > Zn^{2+} > Fe^{3+} > Al^{3+}$. That is, Cu^{2+} ions chelation by the $A\beta_{1-16}$ peptide leads to a complex that by virtue of conformational and surface physical changes becomes less prone to associate and dissociate from the α-HL protein pore. Peptide complexation by Fe^{3+} or Al^{3+} ions, on the other hand, leaves the ability of the peptide to associate reversibly with the protein pore almost un-changed, which is indicative of a very low affinity of such metals to the peptide.

The presented results are in good agreement with recent data demonstrating that the topology of $A\beta_{1-16}$ chelated with the Al^{3+} ion remains preserved, as compared to the Al^{3+}—free peptide (Narayan et al. 2013), while other study performed with the $A\beta_{1-28}$ fragment, revealed that no measurable amounts of $A\beta_{1-28}$–Al^{3+} or $A\beta_{1-28}$–Fe^{3+} adducts are present upon peptide-metal mixing, regardless of experimental conditions (Valensin et al. 2011). Our interpretation of the particular signature of 'metal-complexed', peptide-induced current blockages, lies in the distinct affinity of the peptide to various metals, which in turn governs the propensity of the peptide to assume conformational changes at a given concentration of the metal, which in the end influences the pattern of the peptide-induced blockages. Thus, by employing specific engineered peptide substrates, it appears compelling the feasibility of single-molecule level detection of metals based on the unique current signatures through the α-HL protein immobilized in a lipid membrane, which ensue following the reversible docking of metal-peptide interactions with the protein.

It should be noted that very early studies have pointed to the fact that in low salt concentrations, α-HL pores display open–closed fluctuations in the presence of di- and trivalent cations present at mM concentrations (see Menestrina 1986, as a representative example). In our experiments, however, the *trans*-side addition of either Al^{3+}, Fe^{3+}, or Zn^{2+} at an aqueous concentration of 200 μM, in the absence of the peptide, was not seen to generate open channel fluctuations through a single α-HL pore of magnitude comparable to that mediated by the peptide-α-HL interactions (Fig. S1). In another previous work, in the presence of Cu^{2+} added in the *trans* or *cis* side of the membrane, small current fluctuations were visible (Mereuta et al. 2012), which were not considered in the kinetic analysis due to their the bumping-like appearance, evidenced through a reduced amplitude and low lifetime. Consequently, during the kinetic analysis we present herein, blockage events reflecting the reversible association of either 'metal-free' or 'metal-complexed' peptides to a single α-HL pore were accurately discerned from the background noise, based on their amplitude and kinetics.

To approach our results in quantitative terms, with the goal of estimating the Cu^{2+} and Zn^{2+} dissociation constant

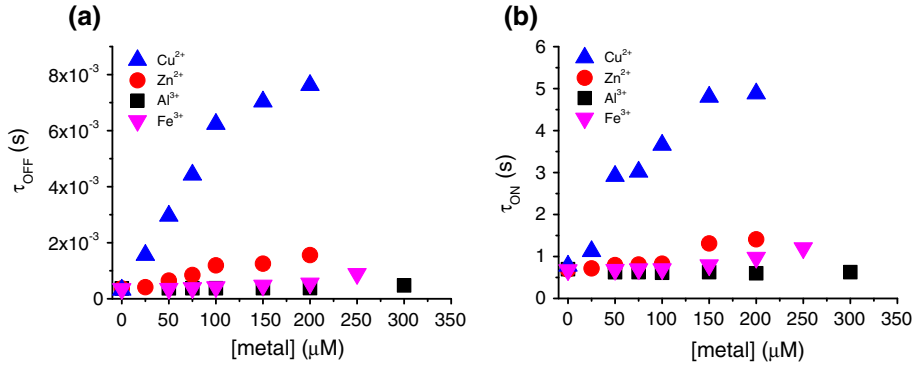

Fig. 4 Statistical analysis of the dissociation (τ_{OFF}; **a**) and association (τ_{ON}; **b**) average dwell time intervals of a single $A\beta_{1-16}$ peptide interacting reversibly with a α-HL pore, measured at various concentrations of the *trans*-added Cu^{2+} (upward triangle; Asandei et al. 2013), Zn^{2+} (*circle*), Al^{3+} (*rectangle*), and Fe^{3+} (*downward triangle*). Throughout experiments, the trans-added $A\beta_{1-16}$ peptide was present at a concentration of 50 μM

values to $A\beta_{1-16}$, we built our rationale on three fundamental facts: (1) while in the absence of metals the $A\beta_{1-16}$ is essentially a random coil in aqueous medium, metal coordination facilitated mainly by the three histidines (i.e., His-6, His-13, and His-14) can induce a conformational change in the peptide that alters its affinity to the protein pore (Tsvetkov et al. 2010; Istrate et al. 2012; Zirah et al. 2006, Mereuta et al. 2012). In the presence of metals, it is thus conceivable that 'metal-free' and 'metal-complexed' peptides are present in the solution, so that the individual blockage events of the ion current through the α-HL protein represent the interaction of the pore with either type of peptides (2) at the concentrations used herein, Cu^{2+}—and Zn^{2+}–$A\beta_{1-16}$ complexes have a 1:1 stoichiometry, namely there is a single binding site for Cu^{2+} and Zn^{2+} on the peptide (Tsvetkov et al. 2010; Istrate et al. 2012; Zirah et al. 2006; Sacco et al. 2012) (3) the 'metal-free' and 'metal-complexed' peptides display distinct kinetic behavior when interacting with the α-HL pore. As conformational changes in $A\beta_{1-16}$ peptides that follow reversible complexation with the metal ions, and metal-peptide binding energy are dependent upon the type on metal bound, it is conceivable that the interaction energy between the 'metal-complexed' $A\beta_{1-16}$ peptide and the α-HL pore, and consequently the association and dissociation reaction constants of the 'metal-complexed' $A\beta_{1-16}$—α-HL vary with the metal type.

To a first approximation, we disregarded in our analysis the buffer influence of the metal-binding affinity to $A\beta_{1-16}$ peptide (Sokołowska and Bal 2005; Sacco et al. 2012). To provide a quantitative understanding of the data shown in Fig. 4, we resorted to a kinetic model we proposed in previous work (Mereuta et al. 2012), which states essentially that the α-HL protein found in its fully open state, denoted by 'O', can associate reversibly with either a 'metal-free' peptide (giving rise to the first type of blockage substate C_1 than could be associated to the relative current block denoted above by $\Delta I_{peptide}$) or with a 'metal-complexed' peptide (giving rise to the second type of blockage substate, C_2, than could be associated to the relative current block denoted above by $\Delta I_{peptide\text{-}metal}$) (see Eq. 1).

$$C_2 \underset{k_4}{\overset{k_3[P-X]}{\leftrightarrow}} O \underset{k_2}{\overset{k_1[P]}{\leftrightarrow}} C_1 \tag{1}$$

In the Eq. (1), $[P]$ and $[P - X]$ denote the available concentrations of the 'metal-free' peptide and 'metal-complexed' peptide, respectively, k_1 and k_3 stand for the association rate constants of the 'metal-free' peptide and 'metal-complexed' peptide with a protein pore initially found in the open state, whereas k_2 and k_4 represent the corresponding dissociation rate constants.

Therefore, for any given initial concentration of the free peptide ($[P_0]$) and metal ($[X_0]$), the analysis of equilibrium binding with both metal and peptide depletion, results in the equilibrium value of the metal-peptide complex $(P - X)_{eq.}$:

$$[P-X]_{eq.} = \frac{([P_0]+[X_0]+K_d)-\sqrt{([P_0]+[X_0]+K_d)^2-4[P_0][X_0]}}{2} \tag{2}$$

where K_d represents the dissociation constant of the reversible peptide (P)—metal ions (X) interaction.

With relevance to our goal of determining K_d values for Cu^{2+} and Zn^{2+}, and as we described before (Mereuta et al. 2012), the theoretical average value of association time intervals measured in-between peptide-generated blockage events of the current through the protein pore (τ_{ON}), caused either by a 'metal-free' peptide (P) or a 'metal-complexed' peptide ($P - X$)), writes:

$$\overline{\tau_{ON}} = \frac{1}{k_3[P-X]_{\text{eq.}} + k_1([P]_{\text{eq.}})} = \frac{1}{k_3[P-X]_{\text{eq.}} + k_1([P_0]-[P-X]_{\text{eq.}})} \quad (3)$$

To arrive at estimations of the K_d values characterizing the various metals—Aβ_{1-16} reversible interactions, which enters expression (3) through the equilibrium value of the metal-peptide complex $(P - X)_{eq.}$ given by (2), we first examined the frequency and duration of the 'metal-free' Aβ_{1-16}—induced current blockades on the ion current through the α-HL pore, at various concentrations of the added peptide (Fig. 1). On the frame of a simple bimolecular interaction between the peptide and the pore, the inverse values of time constants corresponding to the free and occupied pore levels provided quantitative estimations of the association ($rate_{ON}$) and dissociation ($rate_{OFF}$) reaction rates that characterize the 'metal-free' Aβ_{1-16}—α-HL reversible interaction. Consequently, the *on* rate constant was obtained from the slope of the linear fit of $rate_{ON}$ versus peptide concentration ($k_1 = 32 \times 10^3 \pm 1.1 \times 10^3$ M^{-1} s^{-1}), while the *off* rate constants was independent of peptide concentration, and by virtue of the simple bimolecular model taken into account, equal $rate_{OFF}$ ($k_2 = 2.6 \times 10^3 \pm 17$ s^{-1}). With these values, and by fitting expression (3) to data shown in Fig. 4, panel b, estimations of dissociation constant values for Cu^{2+} and, respectively, Zn^{2+} binding to Aβ_{1-16} were obtained ($K^{2+}_{d,Cu} = 4.5 \times 10^{-7}$ M, and $K^{2+}_{d,Zn} = 9.2 \times 10^{-5}$ M) (see also Fig. S2), which are qualitatively similar to values reported in the literature through other techniques (Danielsson et al. 2007; Hong et al. 2010; Tsvetkov et al. 2010). It should be kept in mind that although previously reported metals affinities toward Aβ peptides seemed to vary appreciably, this can be accounted for by taking into considerations distinct experimental conditions (e.g., models used to offset the various buffers influence on metals binding, initial aggregation state of the peptide) (Wärmländer et al. 2013).

Conclusions

Our results demonstrate the potential of the single-molecule level kinetic analysis of metals–Aβ interaction, based on the unique current signatures through the α-HL protein immobilized in a lipid membrane which ensue following the reversible docking of 'metal-free' and 'metal-bound' Aβ_{1-16} with the α-HL protein. The kinetic analysis of the frequency of blockage events entailed by Aβ_{1-16}—α-HL interactions in the presence of metals with augmented affinity toward the peptide (e.g., Cu^{2+} and Zn^{2+}), allowed us to quantify dissociation constants of Cu^{2+} and Zn^{2+} binding to the peptide. Given that metal ions are known to play a critical role in β-amyloid neurotoxicity, investigations into the formation of metal–Aβ complexes are of paramount interest, and easier to implement biophysical techniques like the one presented herein, may be productive in the study of biochemical aspects of metals binding to amyloid peptides. Our findings suggest that the presented technique should be able to complement analytical approaches aimed at unraveling the kinetics of various metals on β-amyloid interactions, and strengthen the feasible emergence of peptide-based metal sensors, through rational functionalizing of nanopores with peptide sequences suited for various metals recruitment and enhanced binding affinity.

Acknowledgments We acknowledge the financial support offered by grants PN-II-ID-PCCE-2011-2-0027, PN-II-PT-PCCA-2011-3.1-0595 and PN-II-PT-PCCA-2011-3.1-0402.

References

Ali FE, Separovic F, Barrow CJ, Yao S, Barnham KJ (2006) Copper and zinc mediated oligomerisation of Aß peptides. Int J Pept Res Ther 12:153–164

Antzutkin ON (2004) Amyloidosis of Alzheimer's A peptides : solid-state nuclear magnetic resonance, electron paramagnetic resonance, transmission electron microscopy, scanning transmission electron microscopy and atomic force microscopy studies. Magn Reson Chem 42:231–246

Asandei A, Apetrei A, Park Y, Hahm KS, Luchian T (2011) Investigation of single-molecule kinetics mediated by weak hydrogen-bonds within a biological nanopore. Langmuir 27:19–24

Asandei A, Schiopu I, Iftemi S, Mereuta L, Luchian T (2013) Investigation of Cu^{2+} binding to human and rat amyloid fragments Aβ (1–16) with a protein nanopore. Langmuir 29(50):15634–15642

Atwood CS, Scarpa RC, Huang X, Moir RD, Jones WD, Fairlie DP, Tanzi RE, Bush AI (2000) Characterization of copper interactions with alzheimer amyloid beta peptides: identification of an attomolar-affinity copper binding site on amyloid beta 1–42. J Neurochem 75:1219–1233

Baran C, Smith GS, Bamm VV, Harauz G, Lee JS (2010) Divalent cations induce a compaction of intrinsically disordered myelin basic protein. Biochem Biophys Res Commun 391:224–229

Bayley H, Luchian T, Shin SH, Steffensen M (2008) Single-molecule covalent chemistry in a protein nanoreactor. In: Rigler R, Vogel H (eds) Single molecules and nanotechnology. Springer Series in Biophysics, Heidelberg, pp 251–277

Chen YR, Huang HB, Chyan CL, Shiao MS, Lin TH, Chen YC (2006) The effect of Abeta conformation on the metal affinity and aggregation mechanism studied by circular dichroism spectroscopy. J Biochem 139:733–740

Chen WT, Liao YH, Yu HM, Cheng IH, Chen YR (2011) Distinct Effects of Zn^{2+}, Cu^{2+}, Fe^{3+}, and Al^{3+} on Amyloid-β stability, oligomerization, and aggregation. Amyloid-β destabilization promotes annular protofibril formation. J Biol Chem 286:9646–9656

Curtain CC, Ali F, Volitakis I, Cherny RA, Norton RS, Beyreuther K, Barrow CJ, Masters CL, Bush AI, Barnham KJ (2001) Alzheimer's disease amyloid-beta binds copper and zinc to generate an allosterically ordered membrane-penetrating structure containing superoxide dismutase-like subunits. J Biol Chem 276:20466–20473

Danielsson J, Pierattelli R, Banci L, Gräslund A (2007) A high-resolution NMR studies of the zinc-binding site of the Alzheimer's amyloid beta-peptide. FEBS J 274:46–59

Drew SC, Barnham KJ (2011) The heterogeneous nature of Cu^{2+} interactions with Alzheimer's amyloid-β peptide. Acc Chem Res 44:1146–1155

Fändrich M (2012) Oligomeric Intermediates in Amyloid formation: structure determination and mechanisms of toxicity. J Mol Biol 421(4–5):427–440

Gu LQ, Shim JW (2010) Single molecule sensing by nanopores and nanopore devices. Analyst 135:441–451

Gu LQ, Braha O, Conlan S, Cheley S, Bayley H (1999) Stochastic sensing of organic analytes by a pore-forming protein containing a molecular adapter. Nature 398:686–690

Hong L, Carducci TM, Bush WD, Dudzik CG, Millhauser GL, Simon JD (2010) Quantification of the binding properties of Cu^{2+} to the amyloid-beta peptide: coordination spheres for human and rat peptides and implication on Cu^{2+}-induced aggregation. J Phys Chem B 114:11261–11271

Hung YH, Bush AI, Cherny RA (2010) Copper in the brain and Alzheimer's disease. J Biol Inorg Chem 15:61–76

Istrate AN, Tsvetkov PO, Mantsyzov AB, Kulikova AA, Kozin SA, Makarov AA, Polshakov VI (2012) NMR solution structure of rat Aβ(1–16): toward understanding the mechanism of rats' resistance to Alzheimer's disease. Biophys J 102:136–143

Karr JW, Akintoye H, Kaupp LJ, Szalai VA (2005) N-terminal deletions modify the Cu^{2+} binding site in amyloid-beta. Biochemistry 44:5478–5487

Kasianowicz JJ, Brandin E, Branton D, Deamer DW (1996) Characterization of individual polynucleotide molecules using a membrane channel. Proc Natl Acad Sci USA 93:13770–13773

Kasianowicz JJ, Robertson JWF, Chan ER, Reiner JE, Stanford VM (2008) Nanoscopic Porous Sensors. Annu Rev Anal Chem 1:737–766

Leal SS, Botelho HM, Gomes CM (2012) Metal ions as modulators of protein conformation and misfolding in neurodegeneration. Coord Chem Rev 256:2253–2270

Majd S, Yusko EC, Billeh YN, Macrae MX, Yang J, Mayer M (2010) Applications of biological pores in nanomedicine, sensing, and nanoelectronics. Curr Opin Biotechnol 21:439–476

Menestrina G (1986) Ionic channels formed by *Staphylococcus aureus* Alpha-Toxin: voltage-dependent inhibition by divalent and trivalent cations. J Membr Biol 90:177–190

Mereuta L, Schiopu I, Asandei A, Park Y, Hahm KS, Luchian T (2012) Protein nanopore-based, single-molecule exploration of copper binding to an antimicrobial-derived, histidine-containing chimera peptide. Langmuir 28:17079–17091

Movileanu L, Schmittschmitt J, Scholtz JM, Bayley H (2005) Interaction of peptides with a protein nanopore. Biophys J 89:1030–1045

Nair NG, Perry G, Smith MA, Reddy VP (2010) NMR studies of zinc, copper, and iron binding to histidine, the principal metal ion complexing site of amyloid-beta peptide. J Alzheimers Dis 20:57–66

Narayan P, Krishnarjuna B, Vishwanathan V, Jagadeesh DK, Babu S, Ramanathan KV, Easwaran KR, Nagendra HG, Raghothama S (2013) Does aluminium bind to histidine? An NMR investigation of amyloid β12 and amyloid β16 fragments. Chem Biol Drug Des 82:48–59

Pagel K, Seri T, von Berlepsch H, Griebel J, Kirmse R, Böttcher C, Koksch B (2008) How metal ions affect amyloid formation: Cu^{2+}- and Zn^{2+}-sensitive peptides. ChemBioChem 9:531–536

Sacco C, Skowronsky RA, Gade S, Kenney JM, Spuches AM (2012) Calorimetric investigation of copper(II) binding to Aβ peptides: thermodynamics of coordination plasticity. J Biol Inorg Chem 17:531–541

Smith DP, Smith DG, Curtain CC, Boas JF, Pilbrow JR, Ciccotosto GD, Lau TL, Tew DJ, Perez K, Wade JD, Bush AI, Drew SC, Separovic F, Masters CL, Cappai R, Barnham KJ (2006) Copper-mediated amyloid-beta toxicity is associated with an intermolecular histidine bridge. J Biol Chem 281:15145–15154

Sokołowska M, Bal W (2005) Cu(II) complexation by "non-coordinating"N-2-hydroxyethylpiperazine-N0-2- ethanesulfonic acid(HEPES buffer). J Inorg Biochem 99:1653–1660

Song LZ, Hobaugh MR, Shustak C, Cheley S, Bayley H, Gouaux JE (1996) Structure of staphylococcal alpha-hemolysin, a heptameric transmembrane pore. Science 274:1859–1866

Stefureac R, Waldner L, Howard P, Lee JS (2008) Nanopore analysis of a small 86-residue protein. Small 4:59–63

Stellato F, Menestrina G, Serra MD, Potrich C, Tomazzolli R, Meyer-Klaucke W, Morante S (2006) Metal binding in amyloid β-peptides shows intra- and inter-peptide coordination modes. Eur Biophys J 35:340–351

Syme CD, Nadal RC, Rigby SE, Viles JH (2004) Copper binding to the amyloid-beta (Abeta) peptide associated with Alzheimer's disease: folding, coordination geometry, pH dependence, stoichiometry, and affinity of Abeta-(1-28): insights from a range of complementary spectroscopic techniques. J Biol Chem 279: 18169–18177

Tougu V, Karafin A, Palumaa P (2008) Binding of zinc(II) and copper(II) to the full-length Alzheimer's amyloid-beta peptide. J Neurochem 104:1249–1259

Tsvetkov PO, Kulikova AA, Golovin AV, Tkachev YV, Archakov AI, Kozin SA, Makarov AA (2010) Minimal Zn(2+) binding site of amyloid-β. Biophys J 99:L84–L86

Valensin D, Migliorini C, Valensin G, Gaggelli E, La Penna G, Kozlowski H, Gabbiani C, Messori L (2011) Exploring the reactions of β-amyloid (Aβ) peptide 1-28 with Al(III) and Fe(III) ions. Inorg Chem 50:6865–6867

Vestergaard M, Kerman K, Saito M, Nagatani N, Takamura Y, Tamiya E (2005) A rapid label-free electrochemical detection and kinetic study of Alzheimer's amyloid beta aggregation. J Am Chem Soc 127:11892–11893

Wang HY, Ying YL, Li Y, Kraatz HB, Long YT (2011) Nanopore analysis of β-amyloid peptide aggregation transition induced by small molecules. Anal Chem 83:1746–1752

Wang G, Wang L, Han Y, Zhou S, Guan X (2014) Nanopore detection of copper ions using a polyhistidine probe. Biosens Bioelectron 53(15):453–458

Wärmländer S, Tiiman A, Abelein A, Luo J, Jarvet J, Söderberg KL, Danielsson J, Gräslund A (2013) Biophysical studies of the amyloid β-peptide: interactions with metal ions and small molecules. ChemBioChem 14:1692–1704

Zirah S, Kozin SA, Mazur AK, Blond A, Cheminant M, Ségalas-Milazzo I, Debey P, Rebuffat S (2006) Structural changes of region 1–16 of the Alzheimer disease amyloid beta-peptide upon zinc binding and in vitro aging. J Biol Chem 281: 2151–2161